Electronic band-structure calculations of some magnetic chromium compounds

VANBRUGGEN, CF; HAAS, C; DEGROOT, RA

Published in:
Journal of Physics%3A Condensed Matter

DOI:
10.1088/0953-8984/1/46/009

J. Phys.: Condens. Matter **1** (1989) 9163–9174. Printed in the UK

Electronic band-structure calculations of some magnetic chromium compounds

J Dijkstra†§, C F van Bruggen†, C Haas† and R A de Groot‡

† Laboratory of Inorganic Chemistry, Materials Science Centre of the University, Nijenborgh 16, 9747 AG Groningen. The Netherlands

‡ Research Institute for Materials, Faculty of Science, Toernooiveld, 6525 ED Nijmegen. The Netherlands

Received 1 March 1989

Abstract. In this paper band-structure calculations of CrS, CrSe, Cr_3Se_4 and CrSb are presented. Together with our accompanying results for the chromium tellurides, these calculations give a coherent picture of the changes in the electronic structure caused by anion substitution and by introduction of cation vacancies. The importance of the Cr–X covalency and the $3d_{z^2}-3d_{z^2}$ overlap of Cr neighbours along the *c* axis is stressed. Further, the band-structure calculations shed some light on the formation, the variation in magnitude and the coupling of the Cr magnetic moments and the indirect magnetic polarisation of the anion bands.

1. Introduction

Binary chromium tellurides show ferromagnetic, metallic behaviour. The electronic structure and some physical properties of $Cr_{1-x}Te$, Cr_3Te_4 and Cr_2Te_3 were presented in the preceding paper (Dijkstra *et al* 1989b, hereafter called I).

Under the above-mentioned chromium tellurides, no half-metallic ferromagnets, i.e. compounds with fully spin-polarised conduction electrons (de Groot *et al* 1983), were found (see I). Besides the majority-spin ($\uparrow$) Cr 3d and Te 5p bands in all cases also a minority-spin ($\downarrow$) band crosses the Fermi level E_F: for CrTe the bottom of the Cr 3d $\downarrow$ band lies below E_F, while in Cr_3Te_4 and Cr_2Te_3 the top of the Te 5p $\downarrow$ band is situated above E_F. One way to create or increase a possible gap at E_F for the $\downarrow$ direction between the Cr 3d and the chalcogen p band is to lower the anion p band. This can be achieved by substitution of Te by Se or S. In this paper the influence on the electronic structure of chemical substitution of Te by Se, S and Sb is studied.

In binary chromium selenides and sulphides, magnetic moments, mainly localised on Cr, are present. The exchange interactions are predominantly antiferromagnetic in these compounds (Goodenough 1963), in contrast to the ferromagnetic chromium tellurides.

The transition from ferromagnetism to antiferromagnetism was studied experimentally for various solid solutions, such as $Cr_{1-\delta}Te_{1-x}Se_x$ (Tsubokawa 1956, Grazhdankina *et al* 1976), $Cr_3Te_{4-x}Se_x$ (Babot *et al* 1973, Babot and Chevreton 1980, Yuzuri

§ Present address: Philips Research Laboratories, PO Box 80000, 5600 JA Eindhoven, The Netherlands

0953-8984/89/469163 + 12 $02.50

Table 1. Crystal parameters (Å) and Wigner–Seitz sphere radii (Å) used in the band-structure calculations of CrS, CrSe, CrSb and CrTe.

	CrS	CrSe	CrTe	CrSb
a axis	3.456[a]	3.684[b]	3.997[c]	4.127[d]
c/*a*	1.667[a]	1.634[b]	1.557[c]	1.321[d]
d(Cr–X)	2.46	2.61	2.78	2.74
d(Cr–Cr)	2.88	3.01	3.11	2.73
r_{Cr}	1.225	1.270	1.223	1.242
r_X	1.740	1.856	2.037	1.973

[a] Chevreton (1964).
[b] Chevreton *et al* (1963).
[c] Makovetskii and Shakhlevich (1978).
[d] Snow (1952).

and Segi 1977), $Cr_3Te_{4-x}S_x$ (Yuzuri and Sato 1987), $Cr_2Te_{3-x}Se_x$ (Yuzuri and Segi 1977) and $CrTe_{1-x}Sb_x$ (Takei *et al* 1966, Grazhdankina and Zaynullina 1970). In many of the above-mentioned solid solutions, canted spin structures are observed.

In § 2 electronic structure calculations of the equi-atomic compounds CrX (X = Te, Se, S and Sb) in the hexagonal NiAs structure are presented. Trends due to the substitution of the anions are analysed and also compared with literature data on MnSb. Further, in § 3 we present the calculated band structure of Cr_3Se_4 and compare it with that of Cr_3Te_4 of I. The magnetic behaviour of metallic $Cr_{3+x}Se_4$ varies from antiferromagnetic for $x > 0$ to metamagnetic or ferromagnetic for $x < 0$ (Maurer and Collin 1980).

2. Compounds with the NiAs structure: CrTe, CrSe, CrS and CrSb

2.1. Introduction

The Cr magnetic moments in CrSe were reported to form an umbrella-like antiferromagnetic spin structure (Corliss *et al* 1961), but later Hollander and van Bruggen (1980) found a trigonal spin structure by neutron diffraction. High-temperature susceptibility data give an extrapolated paramagnetic Curie–Weiss temperature $\Theta = -185$ K and $\mu_{eff} = 4.5\ \mu_B$ (Lotgering and Gorter 1957, Tsubokawa 1960). Specific heat measurements locate the Néel temperature T_N at 320 K (Tsubokawa 1960).

NiAs-type $Cr_{1-x}S$, which always has a few per cent Cr vacancies, exists only above 350 °C. When cooling below this temperature a Jahn–Teller distortion around $Cu^{2+}(d^4)$ results in a monoclinic lattice (Jellinek 1957). High-temperature susceptibility data above 900 K give $\Theta = -1585$ K and $\mu_{eff} = 5.24\ \mu_B$ (Popma and van Bruggen 1969).

CrSb is a metallic antiferromagnet, consisting of ferromagnetic planes perpendicular to the *c* axis, which are antiferromagnetically coupled. The magnetic moment per Cr atom is $2.7\ \mu_B$ (Snow 1952), determined by neutron diffraction. The Curie–Weiss law gives $\Theta = -625$ K and $\mu_{eff} = 3.89\ \mu_B$ (Takei *et al* 1963).

Band-structure calculations, using the augmented spherical wave (ASW) method, were performed for CrS, CrSe and CrSb in the hexagonal NiAs structure for the ferromagnetic, antiferromagnetic and non-magnetic state. The crystal parameters and Wigner–Seitz sphere radii used in the calculation are tabulated in table 1. Details of the

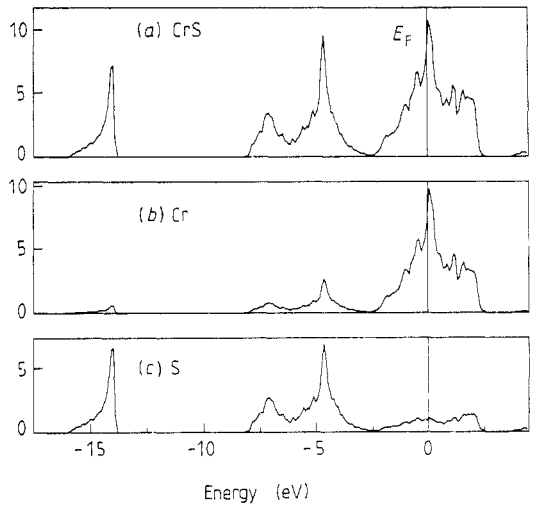

Figure 1. (a) Total density of states (DOS) of non-magnetic CrS. (*b*) Partial Cr DOS. (*c*) Partial S DOS. Units: states/(eV unit cell).

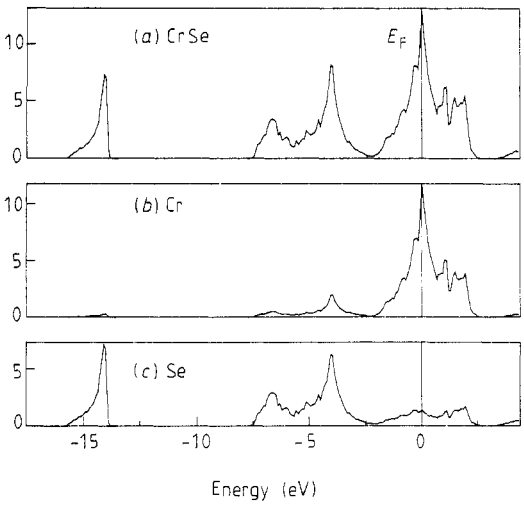

Figure 2. The total and partial DOS of non-magnetic CrSe.

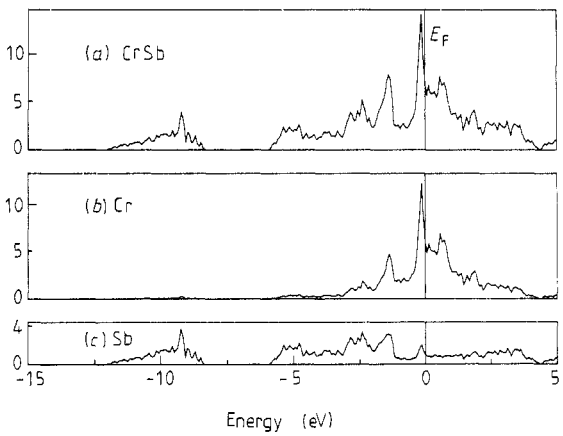

Figure 3. The total and partial DOS of non-magnetic CrSb.

calculation are the same as for CrTe (see I). For comparison also the results for MnSb, isoelectronic with CrTe, CrSe and CrS, obtained by Coehoorn *et al* (1985) and Motizuki *et al* (1986) are given. MnSb is a ferromagnetic metal with a Curie temperature T_C of 585 K and a saturation magnetic moment of 3.5 μ_B per Mn atom.

2.2. *The non-magnetic state*

The calculated densities of states (DOS) of non-magnetic CrS, CrSe and CrSb are shown in figures 1–3, together with the partial contributions from the constituent atoms. The DOS of non-magnetic CrTe is shown in figure 8 of I. The calculated band structure of non-magnetic CrSb (figure 3) is in reasonable agreement with the results of the APW calculation of Motizuki *et al* (1986).

All DOS curves show a low-lying anion s band. The lower part of the d–p complex of 16 bands has mainly anion p character, while contributions of the Cr 3d atoms are predominant in the higher-energy part. Strong covalent mixing between the cation 3d and the anion p states is observed. As in CrTe, the structure of the cation 3d bands is determined by:

(i) the Cr–X covalency; the (trigonally distorted) octahedral coordination of Cr by the anions causes a ligand-field splitting of the 3d states in six non-bonding t_{2g} bands and four antibonding e_g bands;

(ii) the metal–metal interactions; especially the Cr $3d_{z^2}$–Cr $3d_{z^2}$ interactions along the *c* axis—the direction of short metal–metal distances—give strong broadening of the bands, which obscure the ligand-field splitting.

The electronegativity variation of the anions is seen in, for instance, the energy difference ΔE(d–p) between the peak in the d band near E_F and the highest peak in the anion p band and is tabulated in table 2. The chalcogenides are clearly more ionic than the antimonides.

The Fermi level of CrS, CrSe, CrTe and MnSb lies at a high peak in the DOS of mainly non-bonding transition-metal 3d states. The calculated density of states at the Fermi

Table 2. Results of band-structure calculations of compounds with the NiAs structure.

	CrTe	CrSe	CrS	CrSb	MnSb
Non-magnetic					
Separation d–p peak (eV)	3.3	4.1	4.8	1.2	1.3[a]
$N(E_F)$ (states/(eV unit cell))	15.2	12.0	9.3	6.6	10.6[a]
Ferromagnetic					
Exchange splitting Cr/Mn 3d (eV)	2.9	2.7	2.5	2.2	3.5[b]
Total magnetisation (μ_B per Cr/Mn)	3.51	3.40	2.84	2.67	3.24[b]
Moment within Cr/Mn sphere (μ_B)	3.29	3.16	2.64	2.71	3.30[b]
Moment within X sphere (μ_B)	+0.22	+0.24	+0.20	−0.04	−0.06[b]
Antiferromagnetic					
Exchange splitting Cr/Mn 3d (eV)	2.8	2.7	2.5	2.4	3.0[b]
Moment within Cr/Mn sphere (μ_B)	3.17	3.00	2.61	2.79	3.16[b]
ΔE(F-AF) (meV/formula unit)	+29	+110	+116	+213	−19[b]

[a] Motizuki *et al* (1986).
[b] Coehoorn *et al* (1985).

level $N(E_F)$ for the non-magnetic state (see table 2) is lower for broader 3d bands, i.e. for crystals with shorter metal–metal distances ($c/2$ and a). The high values of $N(E_F)$ give rise to ferromagnetism or antiferromagnetism in these compounds.

2.3. The ferromagnetic and antiferromagnetic state

Ferromagnetism is found in CrTe and MnSb and antiferromagnetism in CrSe, CrS and CrSb. Band structures of these compounds were calculated for the ferromagnetic (F) and antiferromagnetic (AF) spin ordering. The same lattice constants and Wigner–Seitz sphere radii were used as in the calculations for the non-magnetic (N) state (table 1). For the antiferromagnetic calculations the spin structure that was found for CrSb (Snow 1952) was used. This structure consists of parallel moments in the basal plane and antiparallel orientation of moments in neighbouring planes along the c axis. The magnetic unit cell is the same as the crystallographic unit cell. The two cations are treated independently in the calculation. The real spin structure in CrSe and CrS is more intricate.

The calculated total and partial DOS of CrS, CrSe and CrSb in the ferromagnetic spin structure are shown in figures 4–6. The DOS of F-CrTe is plotted in figure 5 of I. The results of the AF calculations are shown in figures 7–9 and for AF-CrTe in figure 7 of I. In the AF structure two magnetic sublattices are formed. In figures 7–9(b) and (c) the majority-spin (↑) and minority-spin (↓) DOS of one sublattice are plotted. The DOS of the other sublattice is identical, only the role of ↑ and ↓ is interchanged.

For the ferromagnetic and antiferromagnetic states the same sequence of anion s and p bands and cation 3d band are observed as in the non-magnetic case. The states with mainly cation 3d character show a clear exchange splitting. The magnetic moments within the Wigner–Seitz spheres are given in table 2. The Cr–X covalency gives rise to a small splitting between the anion ↑ and ↓ p bands, which does not exceed 1 eV.

The DOS calculated for the AF structure shows narrower Cr 3d bands than for the F and N state. The t_{2g}–e_g ligand-field splitting of the octahedrally surrounded cation is—especially in the ↓ DOS—more clearly observed than in the N and F situations, since the overlap of $3d_{z^2}$ orbitals between neighbours along the c direction in the AF case gives less broadening of the 3d bands than in the N and F case. This is not caused by a smaller

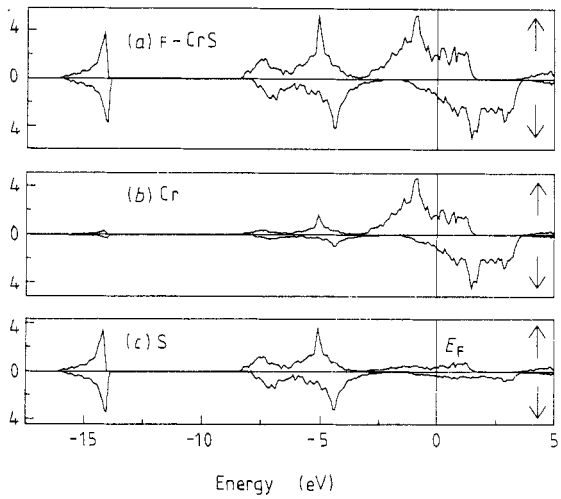

Figure 4. (a) Total density of states (DOS) of ferromagnetic CrS for majority (↑) and minority (↓) spin. (b) Partial Cr DOS. (c) Partial S DOS. Units: states/(eV unit cell).

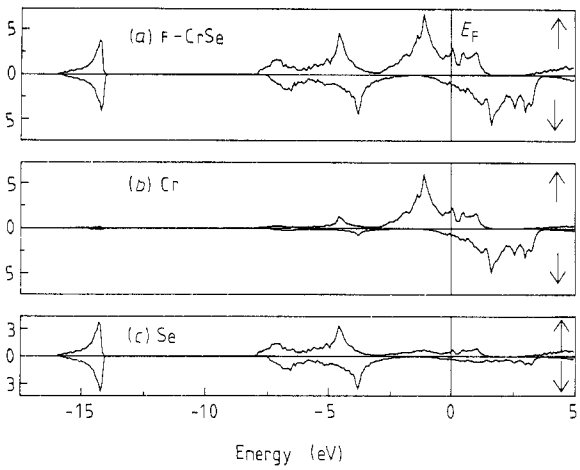

Figure 5. The total and partial DOS of ferromagnetic CrSe.

overlap of the $3d_{z^2}$ orbitals, but merely by the energy position of the interacting states. In the F and N situation states of nearest neighbours along *c* have the same energy. So interaction leads to broadening of these bands. In the AF situation electrons of the same spin direction on neighbouring cations along *c* belong to the majority-spin direction on one and to the minority-spin direction on the other atom. The energy difference between these states is the exchange splitting of about 3 eV, so that the 3d–3d band broadening effect is smaller in the antiferromagnetic ordering. In the AF case the 3d–3d interactions lead to a small rigid shift rather than to a broadening of the 3d bands.

2.4. Discussion

In table 2 some results of the band-structure calculations are tabulated. Results for MnSb (Coehoorn *et al* 1985, Motizuki *et al* 1986) are also included for comparison. The exchange splitting between the metal 3d ↑ and ↓ peaks increases with increasing magnetic moment within the transition-metal sphere (see table 2). The magnetic moments are mainly localised within the transition-metal Wigner–Seitz spheres. Changing the magnetic order leads to a variation of less than 6% of the magnetic moment within the transition-metal spheres. In pure 3d transition metals the calculated magnitude of the magnetic moment is much more strongly dependent on the imposed magnetic structure (Gelatt *et al* 1983), while in Heusler alloys, with larger distances between 3d transition-metal atoms, the calculated magnetic moments differ by not more than 3% for various magnetic orderings (Kübler *et al* 1983). The exchange splitting between the Cr 3d ↑ and ↓ peaks increases with increasing magnetic moment within the transition-metal sphere (see table 2).

In the F ordering the hybridisation of the transition-metal 3d states with the anion p states causes a positive magnetic polarisation of the anion in the chalcogenides and a negative polarisation in the antimonides. Owing to the small electronegativity difference in the antimonides—see ΔE (d–p) for the non-magnetic case in table 2—the centre of mass of the 3d states is well below the top of the Sb 5p band. As a consequence of the d–p covalency some Sb 5p ↑ states are pushed above E_F, leading to a negative magnetic polarisation on Sb. For the chalcogenides the metal 3d states lie above the chalcogen p band. In this case, d–p covalency pushes the p ↑ states to somewhat lower energy than

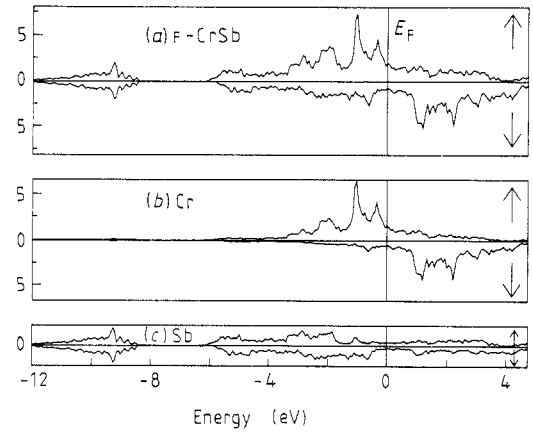

Figure 6. The total and partial DOS of ferromagnetic CrSb.

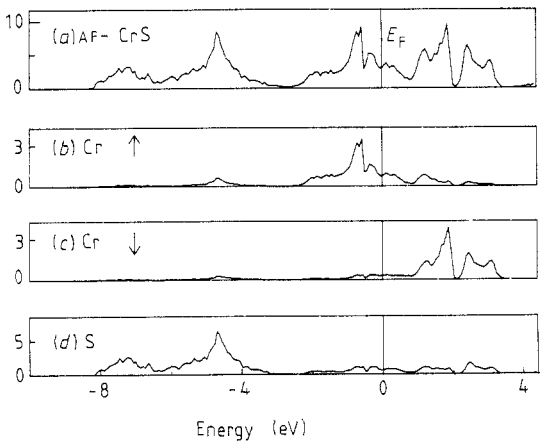

Figure 7. (*a*) Total DOS of antiferromagnetic CrS. (*b*) Sublattice A: ↑ Cr DOS. (*c*) Sublattice A: ↓ Cr DOS. (*d*) Partial S DOS. Units: states/(eV unit cell).

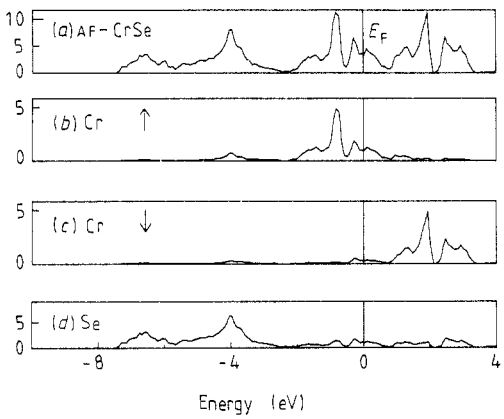

Figure 8. The total and partial DOS of antiferromagnetic CrSe.

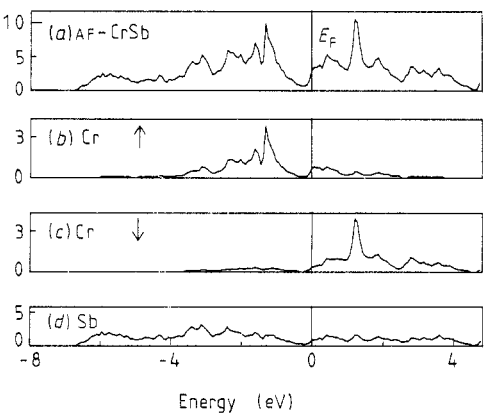

Figure 9. The total and partial DOS of antiferromagnetic CrSb.

the p ↓ states, resulting in a positive magnetisation of the chalcogen atoms. In the AF ordering the magnetic moments within the anion spheres are zero by symmetry.

In principle it is possible to derive values for the exchange constants from the differences in total energies, when calculations are made for several spin orderings (Kübler *et al* 1983). To obtain the first three exchange constants one has to perform calculations for four different spin structures. We have only performed band-structure calculations for two different magnetic structures (collinear ferromagnetic and collinear antiferromagnetic), since other possible magnetic structures for the hexagonal NiAs structure are non-collinear and thus much more difficult to calculate. Recently the first self-consistent band-structure calculation of a non-collinear ferromagnetic compound was published (Kübler *et al* 1988). In table 2 the calculated difference in total energy between the collinear ferromagnetic and antiferromagnetic state ΔE(F-AF) is given; a negative value of ΔE(F-AF) means that the total energy of the ferromagnetic state is lower than that of the antiferromagnetic state.

For the antimonides the calculations give the lowest energy for the true magnetic structure: antiferromagnetic for CrSb and ferromagnetic for MnSb. In these cases the largest exchange splittings and the largest magnetic moments (see table 2) are found for the experimentally observed magnetic structure.

One is inclined to think that in general the magnetic structure with the larger magnetic moments will be the one with the lowest total energy, since larger magnetic moments are attended by a larger exchange splitting, giving the maximum gain in exchange energy. However, for Heusler X_2MnY alloys it was shown that there is a competition between energy gained by inter-sublattice hybridisation (Mn–Y–Mn) and exchange energy, because stronger inter-sublattice hybridisation generally reduces the local magnetic moments (Kübler *et al* 1983).

In the Cr monochalcogenides the experimentally observed magnetic structures are all non-collinear (see § 2 and I), but the calculated energy differences between the ferromagnetic and the antiferromagnetic state show the right trend in the magnetic ordering of these compounds: the absolute value of ΔE(F-AF) increases in the series CrTe–CrSe–CrS, indicating a growing trend to antiferromagnetic ordering in this series. This is in accordance with measurements of the paramagnetic susceptibility. The extrapolated Curie–Weiss temperature Θ is a measure for the overall sign and magnitude of the exchange constants (positive Θ, F; negative Θ, AF): CrTe, Θ = 340 K (Lotgering and Gorter 1957); CrSe, Θ = −185 K (Lotgering and Gorter 1957); CrS, Θ = −1585 K (Popma and van Bruggen 1969). However, the positive sign of the calculated ΔE(F-AF) for CrTe is not in agreement with the observed ferromagnetic character.

From table 2 one can see that larger magnetic moments are found for the F ordering than for the AF ordering. The magnitude of the local magnetic moments is mainly determined by the d–p covalency, although metal–metal interactions also contribute. So, the gain in exchange energy is largest in the ferromagnetic ordering due to d–p covalency.

The decrease in the magnetic moment on Cr in the series Te–Se–S is mainly due to the change in Cr 3d–3d interactions. The Cr 3d–3d interactions are strongest in the compound with the shortest *c* axis, i.e. in CrS, as will be shown below. In the F case the metal–metal interactions, especially the overlap of Cr $3d_{z^2}$ states along the *c* axis, *broaden* the 3d bands, pushing some antibonding 3d ↑ bands above E_F and some bonding 3d ↓ bands below E_F (see figures 4 and 5 and figure 5 of I), leading to a decrease of the magnetic moment well below the ionic value of 4 μ_B. In the AF ordering Cr $3d_{z^2}$ overlap along the *c* axis couples states of the same spin direction. However, these states belong to the majority-spin direction on one and to the minority-spin direction on the

neighbouring Cr atom along the *c* axis. Consequently, mixing of these states due to $3d_{z^2}$ overlap along the *c* axis also gives in the AF ordering a decrease of the magnetic moment. However, the centre of mass of the (occupied) d ↑ band is slightly lowered due to $3d_{z^2}$ overlap, which is not the case in the ferromagnetic ordering. The net effect of the Cr $3d_{z^2}$ overlap along the *c* axis thus benefits the AF ordering, which is therefore found in the compounds with the shortest *c* axis: CrS and CrSe. At larger metal–metal distances, in CrTe, the ferromagnetism due to d–p hybridisation prevails.

3. $Cr_{3+x}Se_4$

In the calculated band structure of Cr_3Te_4 there is no gap between the Cr 3d ↓ and the Te 5p ↓ bands bands and both cross the Fermi level (see figure 9 of I). Substitution of Te by Se might lead to the situation that the anion p ↓ bands no longer cross E_F and a half-metallic ferromagnetic compound would be the result. Experimental studies on the $Cr_3Te_{4-x}Se_x$ ($0 \leq x \leq 4$) system show a gradual change from ferromagnetic to antiferromagnetic behaviour with increasing x (Babot *et al* 1973, Yuzuri and Segi 1977). However, the magnetic properties of $Cr_{3+x}Se_4$ ($-0.2 < x < +0.2$) are strongly dependent on the stoichiometry (Maurer and Collin 1980): antiferromagnetic for $x > 0$ and metamagnetic or ferromagnetic for $x < 0$.

The band structure of Cr_3Se_4 is calculated with ferromagnetic spin ordering. The crystal structure of Cr_3Se_4 can be described in the space group I2/m or C_{2h}^3 (Bertaut *et al* 1964), with the atoms on the special positions:

$$(0, 0, 0), (\tfrac{1}{2}, \tfrac{1}{2}, \tfrac{1}{2}) +$$

2 Cr_1 in (2*c*) $\pm(0, 0, \tfrac{1}{2})$

4 Cr_2 in (4*i*) $\pm(x, 0, z)$ with $x = 0.028$ and $z = 0.240$

4 Se_1 in (4*i*) $\pm(x, 0, z)$ with $x = 0.336$ and $z = 0.866$

4 Se_2 in (4*i*) $\pm(x, 0, z)$ with $x = 0.329$ and $z = 0.879$.

Table 3. Crystal parameters (Å) (Bertaut *et al* 1964) and Wigner–Seitz sphere radii (Å), used in the band-structure calculation of F-Cr_3Se_4.

a axis	3.62
b axis	6.32
c axis	11.77
$x(Cr_2)$	0.028
r_{Cr}	1.217
r_{Se}	1.840
$r_{emptysphere}$	1.217

The Cr_1 atoms are located in the vacancy layers and have two Cr_2 neighbours along the *c* axis. The Cr_2 atoms, located in the fully occupied metal layers, have only one neighbour along the *c* axis, a Cr_1. The cell parameters and Wigner–Seitz sphere radii used in the calculation are given in table 3. The energy band structure is plotted in figure 10. The total and partial DOS of F-Cr_3Se_4 are shown in figure 11. Magnetic moments of 3.250 and 3.144 μ_B within the Cr_1 and Cr_2 Wigner–Seitz spheres, respectively, and of +0.143 and +0.060 μ_B within the Se_1 and Se_2 spheres are calculated. The total magnetisation is 19.89 μ_B per unit cell (6 Cr).

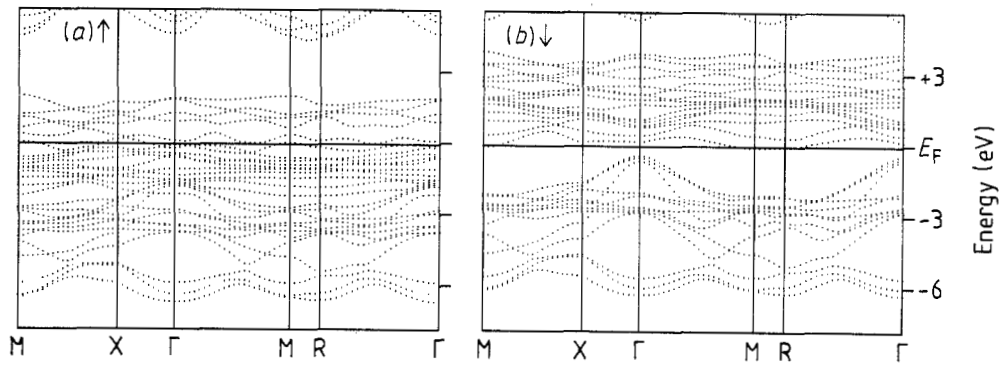

Figure 10. The energy band structure of F-Cr_3Se_4.

The top of the Se 4p band has a small positive spin polarisation, caused by the Cr–Se covalency. The mean value of magnetisation on a Se atom is $+0.10\,\mu_B$. In Cr_3Te_4 a moment of $-0.04\,\mu_B$ was found on the anion. This difference is caused by the larger electronegativity difference in the selenide compound, so that the d/p hybridisation of Cr_3Se_4 is more or less as in figure 13(*a*) of I, while figure 13(*b*) of I applies to Cr_3Te_4.

While in F-Cr_3Te_4 (I, § 4) the Cr 3d ↓ and the Te 5p ↓ bands are overlapping (~0.5 eV), in F-Cr_3Se_4 an indirect gap is opened between the Cr 3d ↓ and the Se 4p ↓ bands with a magnitude of 0.25 eV. All Se 4p ↓ bands lie below E_F. The Fermi level, however, crosses the bottom of the Cr 3d ↓ band. Consequently the magnetisation is

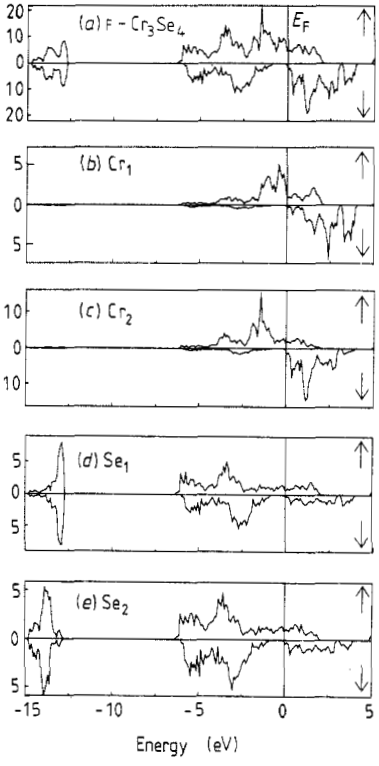

Figure 11. (*a*) Total DOS of ferromagnetic Cr_3Se_4. (*b*) Partial Cr_1 DOS. (*c*) Partial Cr_2 DOS. (*d*) Partial Se_1 DOS. (*e*) Partial Se_2 DOS. Units: states/(eV unit cell).

reduced to a value lower than the 20 μ_B that would have been the result if E_F had fallen in the d/p($\downarrow$) gap. The bottom of the Cr 3d band mainly consists of bonding combinations of the Cr $3d_{z^2}$ orbitals.

The large variations in the magnetic properties of $Cr_{3+x}Se_4$ ($-0.2 \leqslant x \leqslant 0.2$) (Maurer and Collin 1980) are probably correlated with the fact that the Fermi level of stoichiometric Cr_3Se_4 is close to the bottom of the Cr 3d $\downarrow$ band. It is not impossible that meta/ferromagnetic $Cr_{3+x}Se_4$ ($-0.2 < x < 0$) is a half-metallic ferromagnet, since lowering of the Cr concentration gives a narrower Cr 3d $\downarrow$ band, but we are not able to calculate the electronic structure of such a non-stoichiometric compound. The trend observed for substitution of Te by Se indicates that a calculation of ferromagnetic trigonal Cr_2Se_3 would possibly result in a half-metallic ferromagnet, since the smaller Cr concentration will result in a narrower Cr 3d $\downarrow$ band, which possibly lies above E_F. However, Cr_2Se_3 is strongly antiferromagnetic. In the system $Cr_2Se_{3-x}Te_x$ antiferromagnetism is dominant in a much larger concentration range than in $Cr_3Se_{4-x}Te_x$ (Yuzuri and Segi 1977).

Another possibility to decrease the Cr 3d $\downarrow$ band width by lowering the number of Cr 3d–Cr 3d interactions along the *c* axis is substitution of part of the Cr atoms by non-magnetic atoms. When half of the Cr atoms in CrSe are replaced by K atoms, in such a way that every second metal layer along the *c* axis is a K layer, we obtain the metamagnetic compound $KCrSe_2$ (Wiegers 1980). This layered compound becomes ferromagnetic when a magnetic field of only 1.3 T is applied (van Bruggen *et al* 1979). Electronic structure calculations show that $KCrSe_2$ in the ferromagnetic state is a half-metallic ferromagnet, i.e. only minority states cross the Fermi level (Dijkstra *et al* 1989a).

Acknowledgment

One of us (RAdeG) wants to thank the Stichting Fundamenteel Onderzoek der Materie for financial support.

References

Babot D and Chevreton M 1980 *J. Solid State Chem.* **35** 141
Babot D, Wintenberger M, Lambert-Andron B and Chevreton M 1973 *J. Solid State Chem.* **8** 175
Bertaut E F, Roult G, Aleonard R, Pauthenet R, Chevreton M and Jansen R 1964 *J. Physique* **25** 582
Chevreton M 1964 *Thesis* Lyon
Chevreton M, Bertaut E F and Jellinek F 1963 *Acta Crystallogr.* **16** 431
Coehoorn R, Haas C and de Groot R A 1985 *Phys. Rev.* B **31** 1980
Corliss L M, Elliot N, Hastings J M and Sass R L 1961 *Phys. Rev.* **122** 1402
de Groot R A, Mueller F M, van Engen P G and Buschow K H J 1983 *Phys. Rev. Lett.* **50** 2024
Dijkstra J, van Bruggen C F, Haas C and de Groot R A 1989a *Phys. Rev. B* at press
Dijkstra J, Weitering H H, van Bruggen C F, Haas C and de Groot R A 1989b *J. Phys.: Condens. Matter* **1** 9141–61
Gelatt C D, Williams A R and Moruzzi V L 1983 *Phys. Rev.* B **27** 2005
Goodenough J B 1963 *Magnetism and the Chemical Bond* (New York: Interscience)
Grazhdankina N P and Zaynullina R I 1970 *Zh. Eksp. Teor. Fiz.* **59** 1896 (Engl. Trans. 1971 *Sov. Phys.–JETP* **32** 1025)
Grazhdankina N P, Zaynullina R J and Bersenev Y S 1976 *Fiz. Tverd. Tela* **18** 3561
Hollander J C T and van Bruggen C F 1980 unpublished
Jellinek F 1957 *Acta Crystallogr.* **10** 620
Kübler J, Höck K-H, Sticht J and Williams A R 1988 *J. Phys. F: Met. Phys.* **18** 469
Kübler J, Williams A R and Sommers C B 1983 *Phys. Rev.* B **28** 1745

Lotgering F K and Gorter E W 1957 *J. Phys. Chem. Solids* **3** 238
Makovetskii G I and Shakhlevich G M 1978 *Phys. Status Solidi* a **47** 219
Maurer A and Collin G 1980 *J. Solid State Chem.* **34** 23
Motizuki K, Katoh K and Yanase A 1986 *J. Phys. C: Solid State Phys.* **19** 495
Popma T J A and van Bruggen C F 1969 *J. Inorg. Nucl. Chem.* **31** 73
Snow A I 1952 *Phys. Rev.* **85** 365
Takei W J, Cox D E and Shirane G 1963 *Phys. Rev.* **129** 2008
—— 1966 *J. Appl. Phys.* **37** 973
Tsubokawa I 1956 *J. Phys. Soc. Japan* **11** 662
—— 1960 *J. Phys. Soc. Japan* **15** 2243
van Bruggen C F, Wiegers G A, Haange R J and Tolsma P 1979 *Int. Conf. Transition Elements (Stuttgart)* Coll. Abstr. VI, p 242
Wiegers G A 1980 *Physica* **99B** 151
Yuzuri M and Sato M 1987 *J. Magn. Magn. Mater.* **70** 221
Yuzuri M and Segi K 1977 *Physica* **86–88B** 891